

## **Development of a Physico-Chemical Process Model to Estimate Crevice Chemistry for Nickel-Based Alloys**

Pavan K. Shukla, Roberto Pabalan, and Xihua He  
Center for Nuclear Waste Regulatory Analyses  
Southwest Research Institute®  
6220 Culebra Road  
San Antonio, Texas 78238-5166  
E-mail: pshukla@swri.org  
Phone: (210) 522-6534

### **ABSTRACT**

Nickel-based alloys, such as Alloy 600 and C-276, exhibit superior localized corrosion resistance compared to iron-based alloys, such as stainless steel. Nickel-based alloys can be susceptible to localized corrosion in the form of crevice corrosion when the corrosion potential is greater than the repassivation potential in a given environment. The severity of localized-corrosion-induced damage on the metal surface is dependent on the evolution of the crevice region chemical environment. In this paper, we present a physico-chemical model to estimate the chemical environment inside a crevice. The model is developed by imposing the mass balance for reacting and non-reacting chemical species, and by imposing charge conservation. The model is solved using a novel iterative method in which the governing equations for potential and chemical species distributions are solved independently. The model is implemented for nickel-based alloys. Model results are presented for different homogeneous and heterogeneous chemical reactions and considering various electrochemical and chemical conditions.

**Keywords:** crevice corrosion, localized corrosion, repassivation potential, charge conservation, potential distribution

### **INTRODUCTION**

Nickel-based alloys, such as Alloy 600 and C-276, exhibit superior localized corrosion resistance compared to iron-based alloys, such as stainless steel. Nickel-based alloys can be susceptible to localized corrosion in the form of crevice corrosion when the corrosion potential is greater than the repassivation potential in a given environment. The severity of localized-corrosion-induced damage on the metal surface is dependent on the evolution of the crevice region chemical environment. Several experimental studies have been conducted to determine the metal dissolution rate in the crevice region.<sup>1-4</sup> However, the experimental studies do not provide a description of the chemical environment that would develop inside a crevice because of the restricted geometry of the crevices. Furthermore, the experimental studies provide only limited term propagation rate data of the localized corrosion front.

Therefore, the life prediction of nickel-based alloy components and structures in which crevice cracks can initiate and propagate remains a major challenge.

Few studies have been conducted to determine the evolution of chemical environment inside a crevice of nickel and nickel-based alloys. Harb and Alkire<sup>5</sup> developed a process model to simulate the dissolution of a hemispherical corrosion pit on nickel in 0.5M NaCl. The model accounted for multiple species in solution, reaction equilibria, migration, and surface kinetics. In particular, the Harb and Alkire model accounted for complexation of nickel with chloride. The model results indicated the build up of nickel and chloride ions inside the pit. Hoffmeister<sup>6</sup> determined the distribution of dissolved oxygen concentration, chloride concentration, and pH of the in-crevice solution. However, Hoffmeister's work was based upon empirical correlations developed from experimental studies. Watson and Postlethwaite<sup>7</sup> developed a physico-chemical process model to determine the chemical environment inside a crevice for Inconel 625 in chloride-containing solutions. Evitts et al.<sup>8</sup> simulated the Watson and Postlethwaite model<sup>3</sup> for Inconel 625 at high temperature to determine the effect of corrosion on the initiation of crevice corrosion.

In this paper, we present a physico-chemical model to determine the chemical environment inside a crevice. The model considers the transport of two non-reacting anionic species into a crevice and also accounts for metal dissolution, water dissociation, and metal hydroxide formation reactions inside the crevice. To the authors' best knowledge, this model has not been presented elsewhere. The model is solved using a novel iterative method in which the governing equations for potential and chemical species distributions are solved independently. The model is implemented for nickel-based alloys. Model results are presented for different homogeneous and heterogeneous chemical reactions and considering various electrochemical and chemical conditions. The description of the model is provided in the next section and the method is described in the subsequent section.

## MODEL

The physico-chemical process model is developed for a rectangular crevice of length  $L$  and width  $a$ . A schematic diagram of the crevice is presented in Figure 1. A nickel-based alloy is assumed to be immersed in a solution containing chloride, nitrate, and sodium ions. It is assumed that the primary metal dissolution reaction in the crevice is the dissolution of nickel, represented by the following chemical equation



and the corrosion current associated with the dissolution of the nickel is given by the following equation

$$i_{\text{Ni}^{2+}} = \bar{i} \exp[\beta(V - \Phi)] \quad (2)$$

where

- $i_{\text{Ni}^{2+}}$  — corrosion current density associated with the dissolution of nickel ( $\text{A}/\text{cm}^2$ )
- $\bar{i}$  — equilibrium current density ( $\text{A}/\text{cm}^2$ )
- $\beta$  — inverse of Tafel slope ( $\text{V}^{-1}$ )
- $V$  — metal potential (V)
- $\Phi$  — solution potential (V)

The dissolved nickel ion hydrolyzes to form nickel hydroxide and hydrogen ions according to the following reversible chemical reaction



The equilibrium constant for the Eq. (3) is represented by the following equation

$$K_{\text{eq},\text{Ni}} = \frac{C_{\text{NiOH}^+} C_{\text{H}^+}}{C_{\text{Ni}^{2+}}} \quad (4)$$

where

- $K_{\text{eq},\text{Ni}}$  — equilibrium constant (mol/cm<sup>3</sup>)
- $C_{\text{NiOH}^+}$  — concentration of NiOH<sup>+</sup> ions (mol/cm<sup>3</sup>)
- $C_{\text{H}^+}$  — concentration of H<sup>+</sup> ions (mol/cm<sup>3</sup>)
- $C_{\text{Ni}^{2+}}$  — concentration of Ni<sup>2+</sup> ions (mol/cm<sup>3</sup>)

The hydrogen ions, produced by Eq. (3), equilibrate with the hydroxyl ion according to the following water dissociation reaction



The equilibrium constant for the water dissociation reaction is by the following equation

$$K_{\text{H}_2\text{O}} = C_{\text{H}^+} C_{\text{OH}^-} \quad (6)$$

where

- $K_{\text{H}_2\text{O}}$  — equilibrium constant for the water dissociation reaction (mol<sup>2</sup>/cm<sup>6</sup>)
- $C_{\text{OH}^-}$  — hydroxyl ion concentration (mol/cm<sup>3</sup>)

The ionic species present in the crevice region are sodium, chloride, nitrate, nickel, nickel hydroxide, hydrogen, and hydroxyl ions. The steady-state concentration distribution of these ionic species in the crevice is represented by the following equation

$$-\nabla \cdot N_k + R_k = 0 \quad (7)$$

where

- $R_k$  — rate of generation of ionic species  $k$  (mol/sec-cm<sup>3</sup>)
- $N_k$  — flux of ionic species  $k$  (mol/sec-cm<sup>2</sup>)

The flux of an ionic species,  $N_k$ , in the solution is represented by the following Nernst-Planck equation

$$N_k = -z_k u_k F C_k \nabla \Phi - D_k \nabla C_k \quad (8)$$

where

- $z_k$  — charge number of species  $k$
- $u_k$  — mobility of species  $k$  (cm<sup>2</sup>/sec-volt)
- $F$  — Faraday constant = 96,486 C/mol
- $\Phi$  — electrolyte potential (volts)
- $D_k$  — diffusion coefficient of species  $k$  (cm<sup>2</sup>/sec)

It is assumed that the concentrations of various species inside the crevice are low enough to invoke the dilute solution approximation. As a result, the diffusion coefficient and mobility of a chemical species  $k$  are related according to the following equation

$$D_k = u_k RT \quad (9)$$

where

$R$  — universal gas constant = 8.3145 J/K/mol  
 $T$  — temperature of the system (K)

It is further assumed that the crevice solution is electrically neutral.

$$\sum_k z_k C_k = 0 \quad (10)$$

The concentrations of sodium, chloride, nitrate, nickel, nickel hydroxide, hydrogen, and hydroxyl ions at the mouth of crevice are assumed to be equal to the bulk solution concentration.

$$C_k = C_{k,bulk} \quad (11)$$

At the end of the crevice, the flux of the nickel ion concentration is given by the following equation

$$N_{Ni^{2+}} \cdot \vec{n} = \frac{i_{Ni^{2+}}}{2F} \quad (12)$$

where  $\vec{n}$  is the outward normal vector. The flux of all other species at the end of the crevice is zero. In this model, it is assumed that no cathodic reaction occurs inside the crevice and the oxygen reduction reaction is the cathodic reaction which occurs outside the crevice as depicted in Figure 1.

### SOLUTION METHOD

Because the width of a crevice is negligibly small compared to the length of a crevice, it is assumed that concentration gradients across the width of the crevice are also negligible compared to along the length of the crevice. This assumption is consistent with the approach Alkire and Siittari<sup>9</sup> adapted to model potential and concentration distributions inside a pit where pit radius was one third of the pit's depth. Under this assumption, the governing equation for concentration distribution Eq. (8) can be rewritten as

$$\nabla \cdot N_k = R_k + \frac{N_{sk}}{a} \quad (13)$$

where

$a$  — width of the crevice (cm)  
 $N_{sk}$  — flux of the species  $k$  at the metal-solution interface (mol/sec-cm<sup>2</sup>)

Note that the operator  $\nabla$  is equal to  $\frac{d}{dx}$  where  $x$  is the distance down the crevice. The flux of the nickel ions at the metal-solution interface in the crevice region is given by the following equation

$$N_{Ni^{2+}} \cdot \vec{n} = \frac{i_{Ni^{2+}}}{2F} \quad (14)$$

where  $\vec{n}$  is the outward normal vector. The flux of all other species at the metal-solution interface is zero.

The diffusion and migration of the ionic species in the crevice region generates current. The total current density is defined by

$$i = F \sum_{k=1}^N z_k N_k \quad (15)$$

and the divergence of the current is given by

$$\nabla \cdot i = \frac{i_{Ni^{2+}}}{2Fa} \quad (16)$$

Insertion of Eqs. (8) and (13) in Eq. (14) yields

$$\nabla \cdot (\kappa \nabla \Phi) + F \sum_{k=1}^N z_k \nabla \cdot (D_k \nabla C_k) = -\frac{i_{Ni^{2+}}}{2Fa} \quad (17)$$

where

$$\kappa = F^2 \sum_{k=1}^N \frac{z_k^2 D_k C_k}{RT} \quad (18)$$

Rearrangement of Eq. (17) yields

$$\kappa \nabla^2 \Phi + \nabla \Phi \cdot \nabla \kappa = -\frac{i_{Ni^{2+}}}{2Fa} - F \sum_{k=1}^N z_k \nabla \cdot (D_k \nabla C_k) \quad (19)$$

Based upon the stoichiometry of homogeneous chemical reactions given by chemical Eqs. (3) and (5), it is recognized that

$$R_{Ni^{2+}} + R_{NiOH^+} = 0 \quad (20)$$

Equation (20) ensures that there is instantaneous equilibrium between nickel and nickel hydroxide ions. Furthermore

$$R_{Ni^{2+}} + R_{H^+} - R_{OH^-} = 0 \quad (21)$$

Equation (21) ensures that the hydrogen ions are in equilibrium with nickel and hydroxyl ions at all instances.

The divergence of flux of nickel and nickel hydroxide ions can be combined to yield

$$\nabla \cdot (N_{\text{Ni}^{2+}} + N_{\text{NiOH}^+}) = \frac{i_{\text{Ni}^{2+}}}{2Fa} \quad (22)$$

and the divergence of flux of nickel, hydrogen, and hydroxyl ions can be combined to yield

$$\nabla \cdot (N_{\text{Ni}^{2+}} + N_{\text{H}^+} - N_{\text{OH}^-}) = \frac{i_{\text{Ni}^{2+}}}{2Fa} \quad (23)$$

The concentration of nickel hydroxide in Eq. (20) is substituted with nickel and hydrogen ion concentration using Eq. (4). Similarly, the concentration of hydroxyl ion concentration in Eq. (21) is substituted with hydrogen ion concentration using Eq. (6).

The non-reacting species are chloride, nitrate, and sodium ions. The divergence of flux of chloride and nitrate ions are given by

$$\nabla \cdot N_{\text{Cl}^-} = 0 \quad (24)$$

and

$$\nabla \cdot N_{\text{NO}_3^-} = 0 \quad (25)$$

The concentration boundary conditions for these governing equations at the mouth of the crevice are given by Eq. (11). The electrolyte potential at the mouth of the crevice is assumed to be zero; that is

$$\Phi = 0 \quad (26)$$

and at the end of the crevice is

$$\kappa \nabla \Phi + F \sum_{k=1}^N z_k D_k \nabla C_k = i_{\text{Ni}^{2+}} \quad (27)$$

Using Eq. (12), the boundary conditions for Eqs. (22) and (23) at the end of the crevice are

$$(N_{\text{Ni}^{2+}} + N_{\text{NiOH}^+}) \cdot \vec{n} = \frac{i_{\text{Ni}^{2+}}}{2F} \quad (28)$$

and

$$(N_{\text{Ni}^{2+}} + N_{\text{H}^+} - N_{\text{OH}^-}) \cdot \vec{n} = \frac{i_{\text{Ni}^{2+}}}{2F} \quad (29)$$

The flux boundary conditions at the end of the crevice for chloride and nitrate ions are

$$N_{\text{Cl}^-} \cdot \vec{n} = 0 \quad (30)$$

and

$$N_{\text{NO}_3^-} \cdot \vec{n} = 0 \quad (31)$$

An iterative procedure is developed to solve Eqs. (19), (22), (23), (24), and (25) and the electroneutrality condition given by Eq. (10), subjected to boundary conditions given by Eq. (11) and

Eqs. (26)-(31). The governing equations are second order ordinary differential equations with fixed boundary values at the mouth and at the end of the crevice. The equations were solved using the two-point boundary values solver function in MATLAB®.<sup>10</sup>

In the initial iteration, first, Eq. (19) is solved for potential distribution inside the crevice subjected to boundary conditions given by Eq. (26) and (27). The concentration distribution of various species inside the crevice is assumed to be equal to the bulk concentration. The solution of Eq. (19) provides distribution of  $\Phi$ ,  $\nabla\Phi$ , and  $\nabla^2\Phi$  inside the crevice. Second, the distributions of concentrations of chloride and nitrate ions are obtained by solving Eqs. (23) and (24) subjected to the boundary conditions given by Eq. (11) and Eqs. (30) and (31). The solution of Eq. (23) and (24) also provides the values of  $\nabla C_{\text{Cl}^-}$ ,  $\nabla C_{\text{NO}_3^-}$ ,  $\nabla^2 C_{\text{Cl}^-}$ , and  $\nabla^2 C_{\text{NO}_3^-}$  along the length of the crevice. Third, the distributions of concentrations of nickel and hydrogen ion concentrations are obtained by solving Eqs. (22) and (23) subjected to boundary conditions given by Eq. (11) and Eqs. (28) and (29). The solution of Eq. (22) and (23) also provides the values of  $\nabla C_{\text{Ni}^{2+}}$ ,  $\nabla C_{\text{H}^+}$ ,  $\nabla^2 C_{\text{Ni}^{2+}}$ , and  $\nabla^2 C_{\text{H}^+}$  along the length of the crevice. Fourth, the distribution of concentrations of nickel hydroxide and hydroxyl ions and  $\nabla C_{\text{NiOH}^+}$ ,  $\nabla C_{\text{OH}^-}$ ,  $\nabla^2 C_{\text{NiOH}^+}$ , and  $\nabla^2 C_{\text{OH}^-}$  are obtained using Eqs. (4) and (6). Fifth, the electroneutrality condition given by Eq. (10) is used to obtain the sodium ion concentration distribution,  $\nabla C_{\text{Na}^+}$  and  $\nabla^2 C_{\text{Na}^+}$  inside the crevice.

In the subsequent iterations, first, Eq. (19) is solved for potential distribution inside the crevice subjected to boundary conditions given by Eqs. (26) and (27). The calculated values of concentration distribution from previous iteration of various species are used to calculate  $\kappa$  in Eq. (19). Similarly, the calculated values of  $\nabla C_k$  and  $\nabla^2 C_k$  from the previous iteration are used to calculate  $\nabla\kappa$  and second term on right hand side of Eq. (19). The second, third, fourth, and fifth steps are repeated to obtain the concentration distributions and  $\nabla C_k$  and  $\nabla^2 C_k$  using the calculated values of  $\Phi$ ,  $\nabla\Phi$ , and  $\nabla^2\Phi$  in the first step. The calculated values of the potentials and concentrations are compared with the previous iteration values. If the absolute difference in potential and concentrations is less than a specified tolerance limit, the iterative procedure is terminated.

## RESULTS

The model is executed for the free corroding condition. Under the free corroding condition, the metal potential, denoted by  $V$ , is equal to zero in Eq. (2). The value of the equilibrium current density ( $\bar{i}$ ), the inverse of the Tafel slope ( $\beta$ ) in Eq. (2), and equilibrium constants ( $K_{\text{eq,Ni}}$ ,  $K_{\text{H}_2\text{O}}$ ) in Eqs. (4) and (6) are provided in Table 1. The value of the equilibrium current density is obtained from experimental data collected for Alloy 22 in 1.0 M NaCl solution. A cyclic polarization curve was obtained for Alloy 22 in the solution according to ASTM G61<sup>11</sup> at 95 °C [203 °F]. The polarization curve is presented in Figure 2. As seen in the figure, the measured current density is independent of potential in the forward scan; however, current density is a strong function of potential in the reverse scan. The data suggested that the metal surface is covered with a passive film while the Alloy 22 sample was anodically polarized in the forward scan. The current density in the reverse scan is a strong function of potential in the reverse scan. This is due to the fact that the original film is no longer in the passive state to protect the metal surface from corrosion. As seen in the figure, the equilibrium current density is approximately equal to  $2 \times 10^{-6}$  A/cm<sup>2</sup> at an electrode potential equal to zero and the calculated value of the inverse of the Tafel slope is  $0.06 \text{ V}^{-1}$ . The values of equilibration constants are adopted from Malki et al.<sup>12</sup> The values of diffusion coefficients of different species are calculated using a chemical thermodynamic simulator<sup>13</sup> and are provided in Table 2. The bulk concentrations of various chemical species are also provided in Table 2.

The model is simulated for a 5-cm [1.97-in]-long and 0.5-mm [197-mils]-high crevice. The calculated values of electrode potential ( $V - \Phi$ ) are presented in Figure 3. As seen in the figure, the electrode potential becomes more cathodic with increasing distance. The electrode potential at the tip of the crevice is 14 mV more cathodic than the mouth of the crevice. The calculated values of the non-reacting chemical species (chloride, nitrate, and sodium) are presented in Figure 4. As seen in the figure, the chloride, nitrate, and sodium ion concentrations increase with distance from the crevice mouth. Note that the ratio of nitrate to chloride ions remains constant throughout the crevice. This observation can be explained by analyzing the governing equations for concentration distribution of chloride and nitrate inside the crevice. Because the divergence of flux of nitrate and chloride ions is zero through the crevice, the steady-state flux of nitrate and chloride ions is constant throughout the crevice, and the transport properties such as mobility and the diffusion coefficient of nitrate and chloride ions have no impact on the steady-state concentration distribution inside the crevice. In fact, the concentration distribution of nitrate and chloride ions is only dependent on the gradient of potential distribution,  $\nabla\Phi$ , inside the crevice.

The concentration of nickel and nickel hydroxide ions as a function of distance is presented in Figure 5. As seen in the figure, the nickel ion concentration increases with distance from the crevice mouth, whereas the nickel hydroxide ion concentration first increases with distance up to 1.0 cm [0.4 in] and then decreases with distance. The nickel ions are generated in the crevice as the potential becomes more cathodic. However, the nickel hydroxide ion concentration is determined by the equilibrium between the nickel, nickel hydroxide, and hydrogen ions.

The concentration of hydrogen and hydroxyl ions as a function of distance is presented in Figure 6. As seen in the figure, the hydrogen ion concentration increases with distance from the crevice mouth, whereas the hydroxyl ion concentration decreases with distance from the crevice mouth. The hydrogen ions are generated as nickel ions react with water to produce nickel hydroxide and hydrogen ions. An increased concentration in nickel ion corresponds to an increase in hydrogen ion concentration. Because the product of hydrogen and hydroxyl ion concentration is constant, the hydroxyl ion concentration decreases with distance from the crevice mouth. This result also indicates that the crevice solution is more acidic than the bulk solution because of generation of hydrogen ions.

## SUMMARY AND DISCUSSION

We have presented a physico-chemical process model for a steady-state chemical environment inside a crevice for nickel-based alloys. The model accounts for one heterogeneous and two homogeneous chemical reactions. The heterogeneous chemical reaction is the dissolution of nickel metal, and homogeneous chemical reactions are the formation of nickel hydroxide and hydrogen and the dissociation of water. The concentration and potential variations along the crevice width are assumed to be negligibly small compared to the crevice length. The governing steady-state equations for the potential and concentration distributions of various species are algebraically simplified and then solved using a novel iterative procedure. The model is simulated for the parameter values listed in Table 1 and 2.

The calculated results are presented in the form of potential and concentration distribution of various species as a function of distance from the crevice mouth. The model results indicate that electrode potential becomes more cathodic along the crevice depth. The calculated potential distribution inside the crevice is consistent with the results presented by Song and Sridhar<sup>14</sup> and Allahar<sup>15</sup>, who showed that the potential becomes more cathodic inside a crevice.

The calculated results also show that the concentrations of non-reacting anionic species (chloride and nitrate) increase with distance from crevice mouth. Note that the ratio of concentration of nitrate to



chloride ions remains constant throughout the crevice length. This result is consistent with the fact that the concentration distributions of nitrate and chloride ions are solely dependent upon the gradient of potential inside the crevice and are independent of the diffusion coefficient and mobility of the ions.

The concentrations of nickel and hydrogen ions increase with distance from the crevice mouth. The nickel hydroxide ion concentration increases with distance from the crevice mouth up to 1.0 cm [0.4 in] and then decreases thereafter. The hydroxyl ion concentration decreases with distance from the crevice mouth. The concentration profile of nickel ion is consistent with the fact that nickel ions are generated by the dissolution of metal throughout the crevice, and nickel ions are transported along the crevice depth to balance the ionic charge accumulated because of increased concentration of chloride and nitrate ions. The increase of hydrogen ion concentration is consistent with the fact that the nickel ions react with water molecules to produce hydrogen ions. Therefore, a high concentration of nickel ions corresponds to a high concentration of hydrogen ions. The concentration of nickel hydroxide ions is determined by the interplay between the equilibrium constant for the reversible reaction between nickel ions and water molecules, and nickel and hydrogen ion concentrations. The concentration of hydroxyl ions decrease throughout the crevice because the dissociation constant for the water is constant throughout the crevice and the hydrogen ion concentration increases with distance from the crevice mouth.

The physico-chemical process model presented in this paper is preliminary. The model does not account for several heterogeneous reactions such as nitrate and hydrogen ion reduction, and dissolution of other chemical species present in a nickel-based alloy. The model also does not account for homogeneous reactions such as complexation between nickel and chloride ions. In addition, the model is simulated for a constant equilibrium current density. It is expected that the equilibrium current density will change as a function of position inside the crevice because of change in the chemical environment and the polarization state. Nonetheless, the model results provide insight into distributions of potential and concentrations inside the crevice.

### **DISCLAIMER**

This paper was prepared to document work performed by the Center for Nuclear Waste Regulatory Analyses (CNWRA<sup>®</sup>) for NRC under Contract No. NRC-02-07-006. The activities reported here were performed on behalf of the NRC Office of Nuclear Material Safety and Safeguards, Division of High-Level Waste Repository Safety. This report is an independent product of the CNWRA and does not necessarily reflect the view or regulatory position of the NRC.

### **ACKNOWLEDGMENTS**

The authors gratefully acknowledge the reviews of Drs. O. Pensado and S. Mohanty, the editorial review of L. Mulverhill, and the assistance of B. Street in the preparation of this manuscript.

### **REFERENCES**

1. X. He and D.S. Dunn, "Crevice Corrosion Penetration Rates of Alloy 22 in Chloride-Containing Waters," *Corrosion*, Vol. 63, pp 145-158, 2007.
2. X. He, D.S. Dunn, and C.S. Csontos, "Corrosion of Similar and Dissimilar Metal Crevices in the Engineered Barrier System of a Potential Nuclear Waste Repository," *Electrochimica Acta*, Vol. 52, pp. 7556-7569, 2007.
3. F. Hua and G. Gordon, "Corrosion Behavior of Alloy 22 and Ti Grade 7 in a Nuclear Waste Repository Environment," *Corrosion*, Vol. 60, pp. 764-777, 2004.

4. N. Priyantha, P. Jayaweera, G.R. Englehardt, A. Davydov and D.D. Macdonald, "Localized Corrosion of Alloy 22 in Sodium Chloride Solutions at Elevated Temperature," *Corrosion*, Vol. 61, pp. 857-871, 2005.
5. J.N. Harb and R.C. Alkire, "Transport and Reaction During Pitting Corrosion of Ni in 0.5M NaCl I. Stagnant Fluid," *Journal of the Electrochemical Society*, Vol. 138, pp. 2594–2600, 1991.
6. H. Hoffmeister, "Modeling Crevice Corrosion of Pure Nickel by Coupling of Phase and Polarization Behavior at Various pH, Chloride, and Oxygen Levels," *CORROSION/2004*, Paper No. 04289, Houston, TX: NACE, 2004.
7. M. Watson and J. Postlethwaite, "Numerical Simulation of Crevice Corrosion of Stainless Steels and Nickel Alloys in Chloride Solutions," *Corrosion*, Vol. 46, pp. 522–530, 1990.
8. R.W. Evitts, M.M.A. Gad, M.K. Watson, J. Postlethwaite, "Crevice Corrosion of Nickel Alloys at Elevated Temperatures: Experimental and Modeling Studies," *CORROSION/93*, paper no. 601. pp. 601:1–601:10, Houston, TX: NACE, 1993.
9. R. Alkire and D. Siitari, "The Location of Cathodic Reaction During Localized Corrosion," *Journal of the Electrochemical Society*, Vol. 126, No. 1, pp. 15–22, 1979.
10. The MathWorks, Inc., "MATLAB Version 7.7.0.471 (R2008b)," Natick, Massachusetts: The MathWorks, Inc., 2008.
11. ASTM International, "Standard Test Method for Conducting Cyclic Potentiodynamic Polarization Measurements for Localized Corrosion Susceptibility of Iron-, Nickel-, or Cobalt-Based Alloys," *ASTM G61-86*, West Conshohocken, Pennsylvania: ASTM International, 2003.
12. B. Malki, T. Souier, and B. Baroux, "Influence of the Alloying Elements on Pitting Corrosion of Stainless Steels: A Modeling Approach," *Journal of the Electrochemical Society*, Vol. 155, No. 12, pp. C583-C587, 2008.
13. OLI Systems, Inc., "A Guide to Using the OLI Software for Version 2.0 of the Analyzers," Morris Plains, New Jersey: OLI Systems, Inc., 2005.
14. F.M.Song and N.Sridhar, "Modeling Pipeline Crevice Corrosion Under a Disbonded Coating with or Without Cathodic Protection Under Transient and Steady State Conditions," *Corrosion Science*, Vol. 50, pp. 70–83, 2008.
15. K. Allahar, "Mathematical Modeling of Disbonded Coating and Cathodic Delamination Systems," Ph.D. dissertation, University of Florida, Florida, Gainesville, 2003.

**TABLE 1**  
**VALUES OF PARAMETERS IN EQS. (2), (4), and (6).**

Parameter	Values
$\bar{i}$ (A/cm <sup>2</sup> )	$2 \times 10^{-6}$
$\beta$ (V <sup>-1</sup> )	0.06
$K_{\text{eq}, \text{Ni}}$ (mol/cm <sup>3</sup> )	$1.38 \times 10^{-13}$
$K_{\text{H}_2\text{O}}$ (mol <sup>2</sup> /cm <sup>6</sup> )	$10^{-20}$

**TABLE 2**  
**DIFFUSION COEFFICIENTS AND BULK CONCENTRATIONS OF**  
**VARIOUS SPECIES IN THE MODEL.**

Species	Diffusion coefficient (cm <sup>2</sup> /sec) at 95 °C	Concentration (mol/L)
H <sup>+</sup>	$17.0 \times 10^{-5}$	$10^{-8}$
OH <sup>+</sup>	$11.9 \times 10^{-5}$	$10^{-6}$
Na <sup>+</sup>	$3.95 \times 10^{-5}$	Estimated using Eq. (10)
Cl <sup>-</sup>	$5.45 \times 10^{-5}$	0.5
NO <sub>3</sub> <sup>-</sup>	$4.86 \times 10^{-5}$	0.1
Ni <sup>2+</sup>	$2.18 \times 10^{-5}$	$10^{-6}$
NiOH <sup>+</sup>	$2.15 \times 10^{-5}$	$10^{-6}$

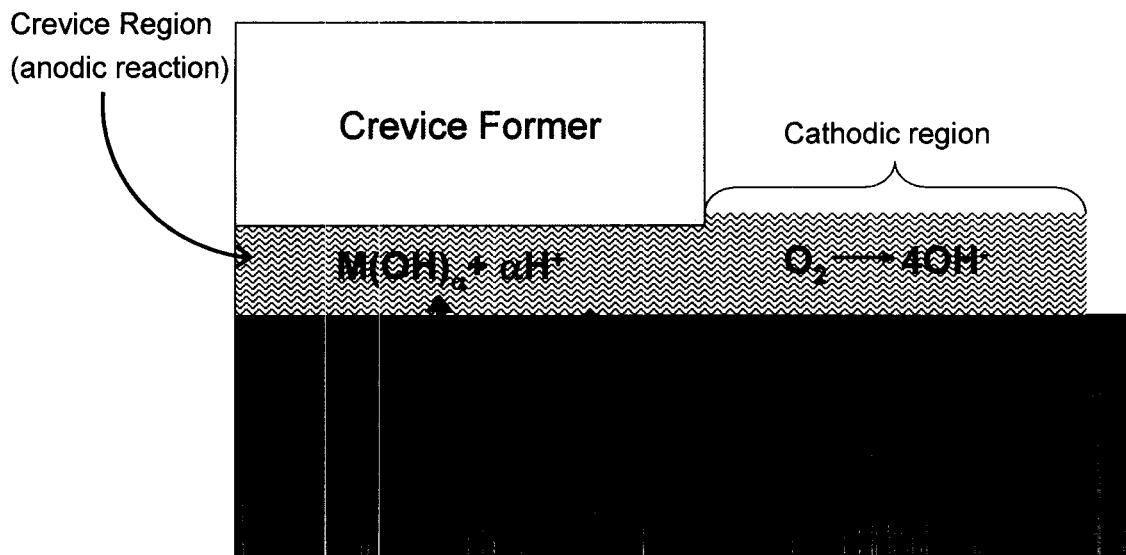


**FIGURE 1 — Schematic Diagram of the Crevice Corrosion Process for a Nickel-Based Alloy. The Anodic Reaction in the Crevice Region is the Nickel Dissolution, Whereas Cathodic Reaction in the Cathodic Region is the Oxygen Reduction.**

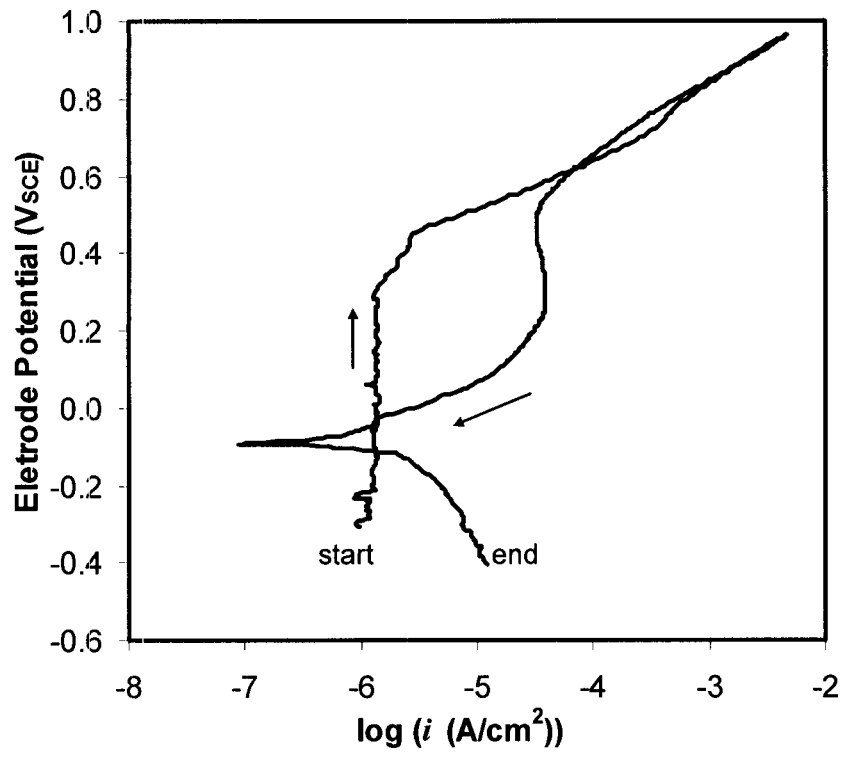


**FIGURE 2 — Potentiodynamic Polarization Curve for Alloy 22 in 1.0 M NaCl Solution at 95 °C [203 °F]**

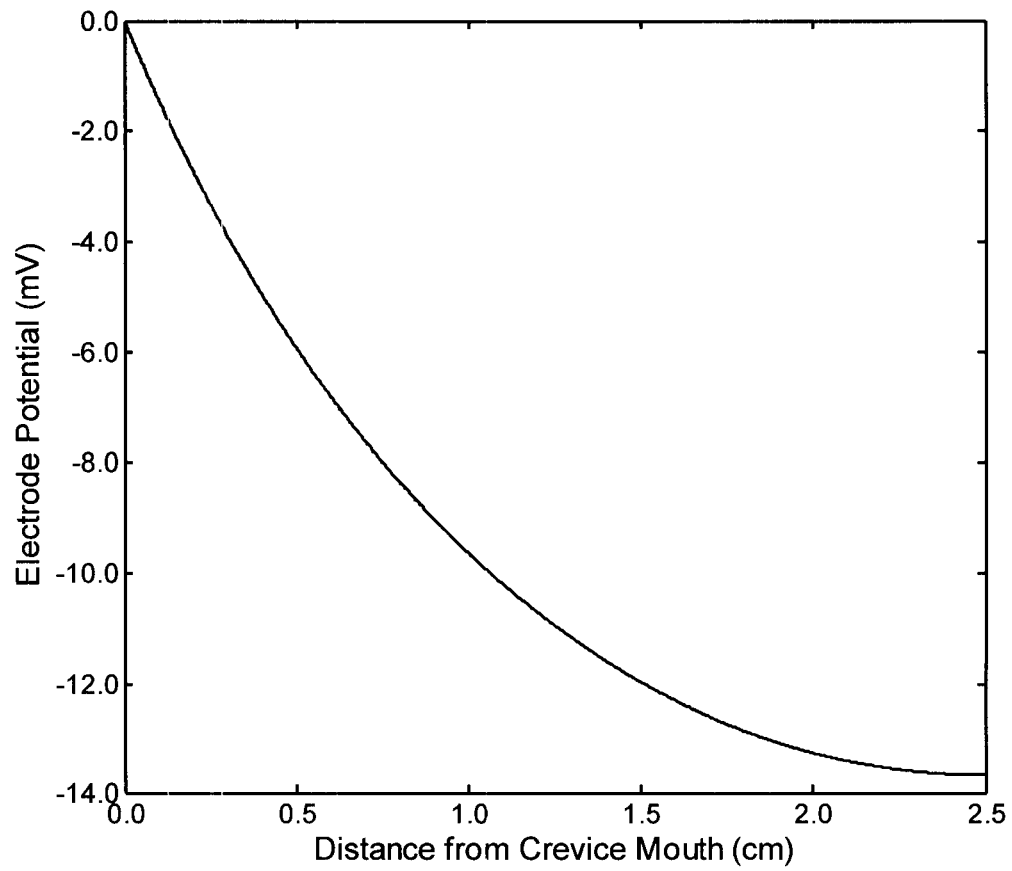


**FIGURE 3 — Electrode Potential ( $V - \Phi$ ) as a Function of Distance From Crevice Mouth**

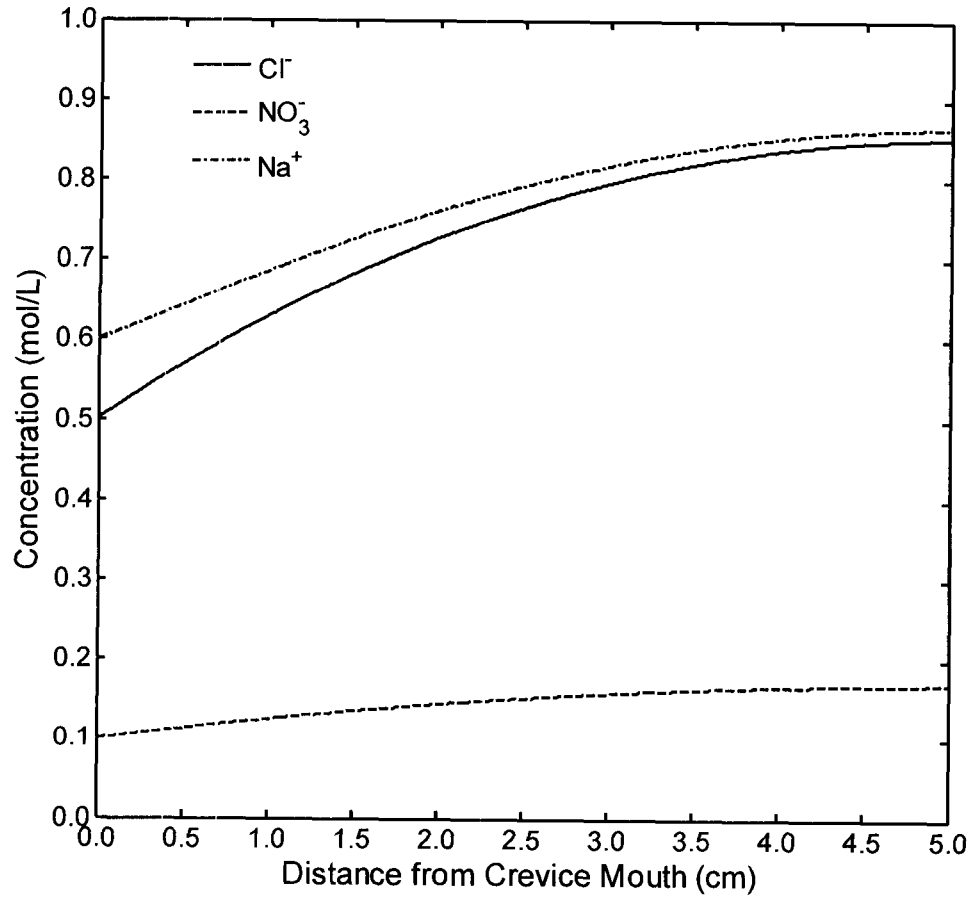


**FIGURE 4 — Concentration of Non-Reacting Species (Chloride, Nitrate, and Sodium) as a Function of Distance From Crevice Mouth**

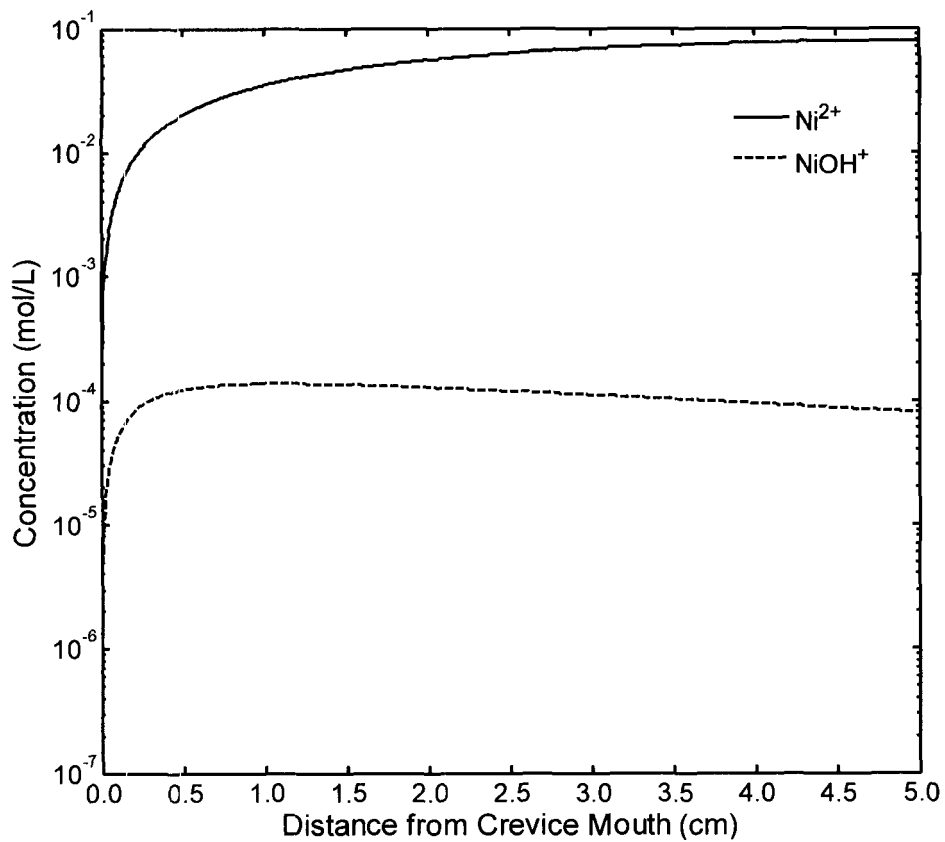


**FIGURE 5 — Concentration of Nickel and Nickel Hydroxide Ions as a Function of Distance From Crevice Mouth**



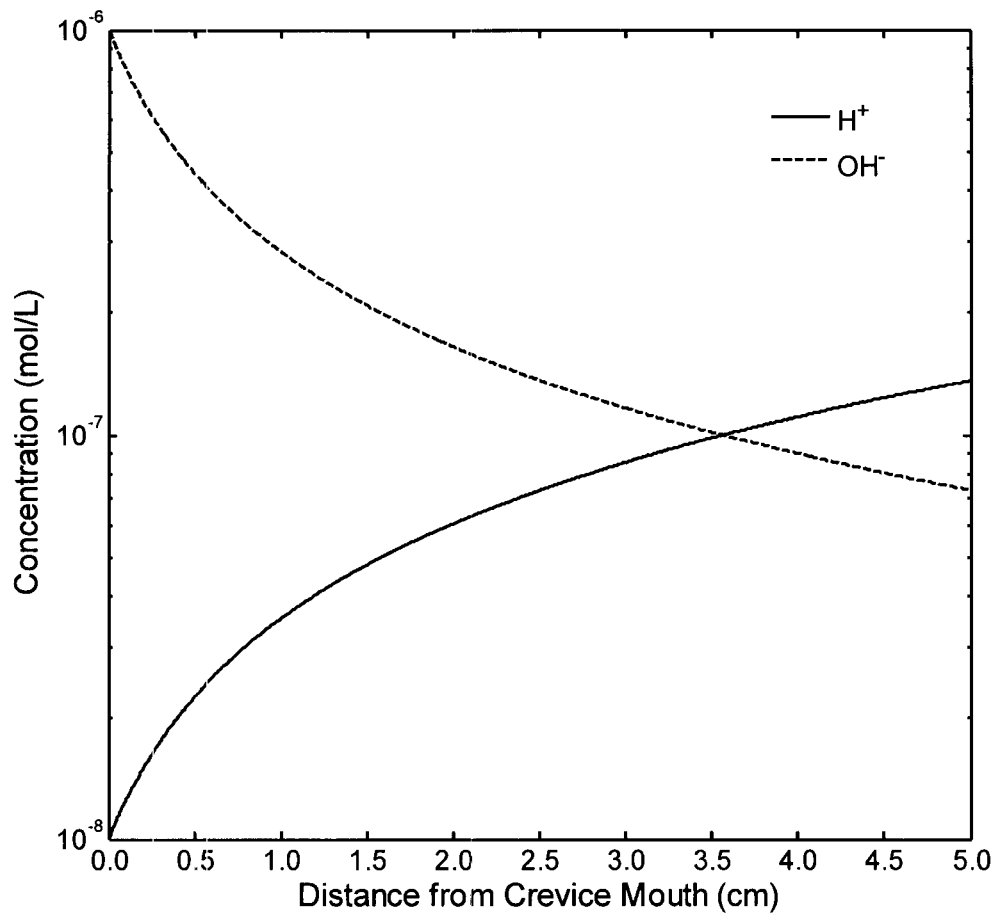


**FIGURE 6 — Concentration of Hydrogen and Hydroxyl Ions as a Function of Distance From Crevice Mouth**